10.1109/16.24367

Deep-Level Transient Spectroscopy of $Al_xGa_{1-x}As$/GaAs Using Nondestructive Acousto-Electric Voltage Measurement

MASSOOD TABIB-AZAR, MEMBER, IEEE, AND FARES HAJJAR

Abstract—**The amplitude and the transient time constant of the acoustoelectric voltage is measured as a function of temperature to determine the activation energy of deep levels in $Al_xGa_{1-x}As$/GaAs grown by molecular-beam epitaxy. In comparison to other methods based on monitoring the capacitance transient, this method has several advantages. The technique is nondestructive, and because of the dependence of the polarity of the acoustoelectric voltage on the carrier type, it yields information about the charge of the transient carriers and the type of deep traps involved in the release or trapping of these carriers. It has also, in particular, large sensitivity in studying high-resistivity materials.**

I. Introduction

It is well known that deep levels play an important role in the operation of $Al_xGa_{1-x}As$/GaAs-based high electron mobility transistors, photodetectors, and light modulators. More specifically, deep levels acting as carrier traps deteriorate the dc bias stability of these devices and limit the impulse response of detectors. Deep levels and their properties are also important parameters in characterizing the material quality.

Deep-level transient spectroscopy (DLTS) is widely used to determine the electrical properties of trap levels in relatively low-resistivity semiconductors [1]. To study high-resistivity materials, other more suitable techniques, such as photoinduced current transient spectroscopy (PICTS) [2], thermally stimulated spectroscopy (TSC) [3], and using the Hall effect [4] have been developed.

The surface acoustic wave (SAW) technique, although somewhat less known, also has been used to study a variety of semiconductors including GaAs and $Hg_xCd_{1-x}Te$ [5]–[10]. Its most important advantages are: 1) it is nondestructive, i.e, it does not require any diode structure; 2) it is extremely sensitive in studying high-resistivity materials; and 3) the carrier type can also be determined. Its main disadvantages are that its results are hard to analyze, and also a tightly controlled environment is required for reproducibility. In studying deep levels in semiconductors, however, it is shown that the results are straightforward, easy to analyze, and reproducible [11]. Here we have applied the SAW technique to study molecular-beam epitaxy (MBE) $Al_xGa_{1-x}As$/GaAs, which is extensively used in fabricating variety of devices including high electron mobility transistors and infrared photodetectors.

In the majority of deep-level measurements, a trap state inside the semiconductor bandgap is filled by an external stimulus, such as an externally applied voltage across a metal-oxide-semiconductor (MOS) structure or an optical pulse directed at the depletion region of an MOS diode. After the external stimulus is removed, the traps emit their charges to move toward their equilibrium state. The rate of emission of charges depends on the trap-state parameters that are themselves temperature dependent. These transients, therefore, are recorded as a function of temperature to extract trap parameters. In traditional DLTS a relatively large background carrier concentration is required to fill the trap states by accumulating forward-bias voltages. The optical DLTS eliminates this restriction by filling the trap states by photo-generated carriers. In both approaches, 1) a diode structure is needed to perform the measurement, and 2) bulk trap states are mainly studied.

In the SAW technique a diode structure is not needed and the transients are studied by directly monitoring the carrier type and concentrations within a few micrometers (depending on the wavelength of SAW and the carrier concentrations) depth of the surface. Also, the sensitivity of the SAW measurement becomes larger as the resistivity of the sample is increased.

The SAW measurement setup is shown in Fig. 1. Radio frequency pulses with typically 55-MHz center frequency, microsecond to millisecond duration and millisecond repetitions are applied to the interdigitated transducers generating SAW at the $LiNbO_3$ surface. The semiconductor sample is placed at the surface of the $LiNbO_3$ delay line, and using a mechanical probe the semiconductor is slightly pressed against the $LiNbO_3$. This mechanical probe is also used as an electrical probe to capacitively detect any voltages that develop across the semiconductor due to the acoustoelectric interaction (AEI). The AEI takes place between the electric field accompanying the SAW and the free carriers of the semiconductor. The AEI results in the modification of the

Manuscript received December 2, 1988; revised February 28, 1989. This work was supported in part by the NASA Lewis Research Center under Grant NAG3-816. The review of this paper was arranged by Associate Editor R. P. Jindal.

The authors are with the Electrical Engineering and Applied Physics Department, Case Western Reserve University, Cleveland, OH 44106.

IEEE Log Number 8927649.

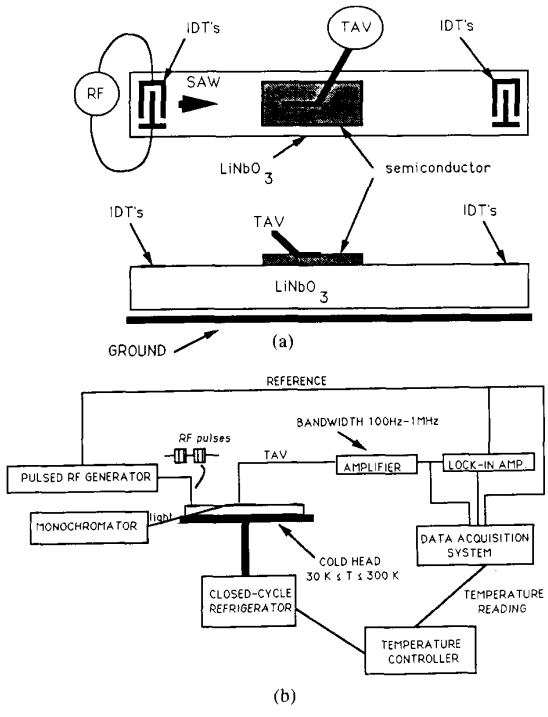

Fig. 1. (a) $LiNbO_3$ delay line. (b) The experimental setup to perform transverse acousto-electric voltage (TAV) versus temperature measurements under different illumination conditions. The Keithley 500 data acquisition system and an IBM system 11/30 are used to monitor and store TAV amplitude and various transient time constants versus temperature.

SAW parameters and the development of dc and harmonics across the semiconductor. The transverse component of the dc voltages, the transverse acoustoelectric voltage (TAV), is extensively used in semiconductor studies [5]–[11]. The longitudinal components are used in carrier mobility determinations [8].

The AEI results in an alteration of the carrier density at the surface of the semiconductor. The rate at which these excess charges are induced at the semiconductor surface, or diminished after the passage of the SAW pulse, can be related to the position, the density, and the cross section of the deep levels inside the bandgap of a high-resistivity semiconductor. The amplitudes and the time constants associated with the TAV waveform are monitored as a function of the temperature to determine the trap parameters.

II. Theoretical Considerations

The most recent treatment of AEI is a work by Fritz [12] who has relaxed some of the simplifying assumptions of other authors except that his treatment applies to highly extrinsic semiconductors. Since the semiconductors that we have dealt with throughout this work are highly intrinsic/compensated samples, we have to reconsider AEI, relaxing some of Fritz's simplifying assumptions. The TAV is related to the carrier concentration and mobility through the following procedure. The modulation in the carrier concentration ($n^{(1)}$) and the electric field ($E^{(1)}$) inside the semiconductor that results due to the passage of the SAW is determined. Then a nonlinear current density (J_{n1}) is defined, and it is used as a source term in the semiconductor constitutive equations to determine the dc signals that develop across the semiconductor

$$J_{n1} = e\mu \langle n^{(1)} E_y^{(1)*} \rangle . \tag{1}$$

We basically follow the derivation of [12] with the exception that we cannot make the simplifying assumption that the Debye length (λ_D) is much less than the inverse of the SAW wave number (k). (The semiconductor that is used in the present study has a carrier concentration of 10^7–10^{10} cm^{-3}, which yields a Debye length larger than 10^{-4} cm. The wavenumber of a 55 MHz ($\omega = 2\pi \times 55$ MHz) SAW traveling at $LiNbO_3$ is 991 cm^{-1} yielding $\lambda_D k$ on the order of unity.)

The J_{n1} that results when the requirement $\lambda_D k << 1$ is relaxed has the following form in slightly n-type materials [11]:

$$J_{n1} = \frac{\mu \epsilon_s \phi^2 k^2 \omega_{cn} \omega_{Dn}}{(\omega_{cn}^2 + (\kappa'^2 + \kappa''^2)\omega^2/k^2)} \cdot \{\alpha \exp(2\kappa' y) + \beta \exp(k + \kappa' y)\} \tag{2}$$

where

$$\alpha = (\kappa'' - \kappa' \omega_{cn}/\omega)\omega_{cn}/\omega \tag{3}$$

and

$$\beta = \{[\kappa'' \sin(\kappa'' y) - \kappa' \cos(\kappa'' y)] - [\kappa' \sin(\kappa'' y) + \kappa'' \cos(\kappa'' y)]\omega_{cn}/\omega\} \tag{4}$$

where

$$\kappa'^2 = [k^2 + \lambda_D^{-2} + \sqrt{(k^2 + \lambda_D^{-2})^2 + \omega^2 \omega_{cn}^{-2} \lambda_D^{-4}}]/2 \tag{5}$$

and

$$\kappa''^2 = [-k^2 - \lambda_D^{-2} + \sqrt{(k^2 + \lambda_D^{-2})^2 + \omega^2 \omega_{cn}^{-2} \lambda_D^{-4}}]/2. \tag{6}$$

In the above equations, ω_{cn} is the dielectric relaxation frequency ($= q\mu_n n/\epsilon_s$, where q is the elementary charge, μ_n is the mobility, n is the electron concentration, and ϵ_s is the dielectric constant), and ω_{Dn} is the diffusion frequency (V_s^2/D_n where V_s is the SAW velocity and D_n is the diffusion coefficient).

The above nonlinear current density differs from the one derived by Fritz and others in high-resistivity materials (with an electron concentration less than 10^{10} cm^{-3} and a mobility of 2000 $cm^2/V \cdot s$ in GaAs). Relaxing the simplifying assumptions of others results in faster decay of the SAW electric field inside the semiconductor. This results in a decay of J_{n1} inside the material that is faster than the decay of J_{n1} derived by others [12].

In Fig. 2 the behavior of the dc excess carrier concentration ($n^{(0)}$), the dc electric field ($E^{(0)}$), the dc acousto-electric potential, and the nonlinear acousto-electric cur-

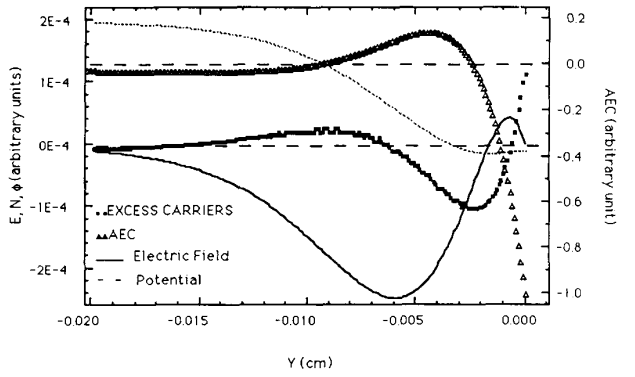

Fig. 2. The electric field (solid line), the potential (dotted line), the excess carrier concentration (squares) and the nonlinear current density (triangles) profiles inside GaAs. The semiconductor is at $y < 0$, and its surface is at $y = 0$.

rent density (J_{n1}) inside the semiconductor are shown. The AEI tends to accumulate the semiconductor surface and to deplete the region beneath the surface. This is an important point that apparently has been overlooked by many investigators; although it was known to us through experimental observations, it was first reported in [12].

Fig. 3 shows the transverse acoustoelectric voltage (TAV), which develops across the semiconductor, as a function of electron concentration [11]. This potential is calculated assuming that it is detected across a semiconductor as an open-circuit voltage. TAV is directly proportional to the carrier concentration in a range that is of interest in the present work, i.e., $10^6 \leq n \leq 10^{12}$ cm^{-3}. Also, as mentioned before, it is negative when the semiconductor is p-type, and it is positive when it is n-type. This property of TAV is used to identify the type of the carriers at the semiconductor surface under different conditions.

Before starting the analysis of the data, it is instructive to model the SAW–semiconductor interaction, which results in the TAV signal. The TAV waveform that develops in response to the SAW pulse is shown in Fig. 4(a). The SAW rise time is on the order of a few nanoseconds (the SAW frequency being 55 MHz). Various rise and fall times associated with the TAV waveform are on the order of 0.01–100 ms. Therefore, as far as the TAV waveform is concerned, the SAW pulse can be treated as a square pulse. Different features of the TAV waveform indicate that a nonlinear process plus a band-pass filtering action take place to transform the SAW pulse into the TAV waveform. Representing the nonlinear process with an ideal diode (with a zero turn on voltage) and the band-pass filter with resistors and capacitors, one gets the simple model shown in Fig. 4(b). It should be noted that since the rise and fall times associated with the positive part of the TAV are different than its negative part, in general, RC's depend on whether the SAW is ON or OFF. At a fixed temperature, τ_1 usually tends to be smaller than τ_2. This is an interesting point to note since it somewhat clarifies the role of AEI in altering the dc surface carrier concen-

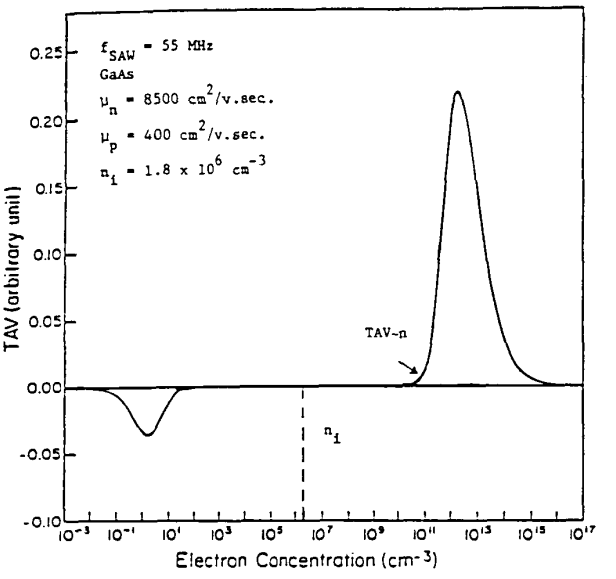

Fig. 3. TAV versus carrier concentration across GaAs at $T = 300$ K and at a SAW frequency of 55 MHz.

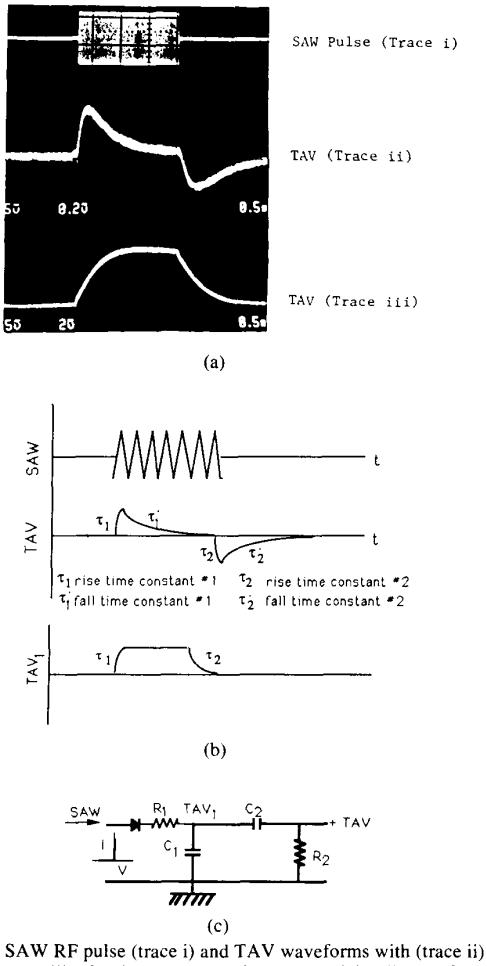

Fig. 4. (a) SAW RF pulse (trace i) and TAV waveforms with (trace ii) and without (trace iii) aluminum ground plane at the delay line surface. (b) A simple circuit model to study SAW–semiconductor interaction.

tration. It indicates that, when SAW is ON, it increases the dc surface conductivity.

Experimentally it is observed that almost always τ_1 is smaller than τ_1'. In qualitative terms, τ_1 is determined, in addition to other geometric parameters, by how fast the nonlinear current density profile can be established. This requires accumulation of the majority carriers at the surface and their depletion beneath the surface. The characteristic time constant associated with these processes is on the order of the dielectric relaxation time constant, which is around 300–400 ns for GaAs with an electron concentration of 10^{10} cm^{-3} and a mobility of 2000 cm^2/V · s. It should be mentioned that, as the semiconductor becomes more intrinsic, the dielectric relaxation time constant becomes larger, and hence, other factors such as generation lifetime of the carriers start contributing to τ_1. The τ_2 also depends on semiconductor parameters as well as the detection scheme used. In Fig. 4(a) two TAV waveforms are shown. These are detected with and without an aluminum ground plane at the $LiNbO_3$ surface. When there is a ground plane, C_2 is very large, and the TAV does not decay appreciably over a few hundred milliseconds. It is quite reasonable, however, to assume that the contribution of the structure to C_2 remains constant as a function of temperature.

Fig. 5 shows the $LiNbO_3$/semiconductor system and various components associated with different parts of that structure. It also shows how various components shown in Fig. 4(c) can be related to the $LiNbO_3$/semiconductor system. $C_2 (= C_{st})$, when the open-circuit detection scheme is used, is very small and it is on the order of 4–5 pF ($C_{st} = \epsilon_p \epsilon_0 A/d$, $\epsilon_p \cong 50$, $A \cong 0.1$ cm^2, and $d \cong 0.5$ mm). In the open-circuit detection scheme the semiconductor bulk resistance (R_{sb}) and the back contact resistance (R_{bc}) can be ignored.

R_1 mainly consists of the space-charge resistance (R_{sc}) of the semiconductor surface within the AEI depth. R_{sc} contains all the interesting information about the semiconductor surface conductivity. In highly intrinsic semiconductors, the majority carriers that are attracted to the surface may come from the semiconductor bulk (with a large response time due to the low dielectric frequency). They may also be generated from deep traps where the cross over between the Fermi level energy and the trap level energy is altered due to the AEI. The R_{sc}, therefore, is a dynamic resistance. It is determined by the resistivity at a given temperature in addition to any generation/recombination of carriers at the deep traps due to AEI. Based on the above considerations, it can be concluded that two factors determine the behavior of the TAV waveform as a function of temperature: 1) thermally stimulated conductivity and 2) recombination/generation at and beneath the semiconductor surface where excess carriers are induced due to AEI. These two factors are dependent on each other. However, as far as the AEI is concerned, the former determines the background carrier density (mobility being a weak function of temperature), and hence, the amplitude of the TAV and the later determine the rise and fall time constants of the TAV waveform.

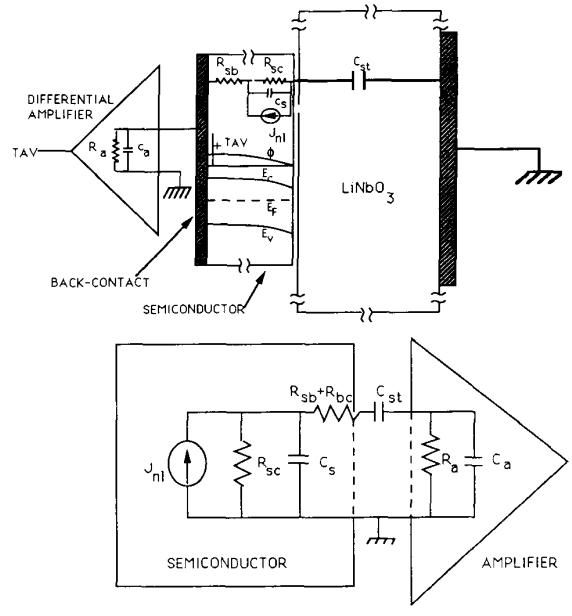

Fig. 5. $LiNbO_3$/semiconductor system and various electrical components associated with it.

It can be shown [13] that, when it is assumed that thermally stimulated carrier concentration reaches maximum when the Fermi level crosses the trap energy (E_T, measured from the conduction band) and in quasi-equilibrium, the trap energy is related to the conductivity peak temperature (T_m) as follows:

$$E_T = 23kT_m \tag{7}$$

where k is the Boltzmann constant and the factor 23 is calculated using typical values for capture cross sections in GaAs. It should be emphasized that (7) is an approximation.

The TAV time constants can be related to the recombination/generation rates as follows. $R_{sc}C_{sc}$ is associated with the space-charge region of the semiconductor surface. Physically it represents how fast the excess carrier profile can be accomplished in response to AEI. This means the downward bending of the bands (weak accumulation) in a slightly n-type semiconductor as shown in Fig. 2. The TAV is a direct measure of this band bending. Treating the AEI as an excitation that results in the accumulation of the semiconductor surface, the release of the majority carriers from deep levels that leads to the achievement of the thermal equilibrium has the following dependence on time [4]:

$$\Delta n(t) = N_t (1 + \tau_f/\tau_g)^{-1} \exp(-t/\tau_g) \tag{8}$$

where N_t is the trap density of those deep levels near the Fermi level, τ_f is the time constant associated with the filling rate of these levels in the presence of the external stimuli, and τ_g is the time constant associated with the release of the carriers from deep levels once the external

stimuli is turned off. Since in high-resistivity materials, as discussed before, TAV is directly proportional to the carrier density at the semiconductor surface, the decay time constant associated with the TAV waveform is a direct measure of τ_g. In the open-circuit detection scheme used in the present work, τ_2 shown in Fig. 4 is the time constant that is closely related to τ_g. Furthermore, τ_g has the following temperature dependence [4]:

$$\tau_g^{-1} = \gamma_n T^2 \sigma_{na} \exp(-E_n/kT) \quad (9)$$

where $\gamma_n = 2.28 \times 10^{20}$ cm^{-2}s^{-1}K^{-2} for electron traps in GaAs, σ_{na} is the apparent cross section, and E_n is trap energy from the conduction band. It should be noted that, since the TAV signal is detected through a high-pass filter (essentially a differentiator), the amplitude of the detected signal also reflects the TAV transient time constants.

Illumination of the semiconductor surface at the AEI region can be used to change the occupancy of the trap levels by establishing quasi-Fermi levels for electrons and holes, respectively, above and below the Fermi level. Using such illumination, the deep levels that are most active in establishing the steady state (after the SAW pulse) can be selected using proper photon energies and/or proper intensities.

III. Experimental Results and Discussion

The $Al_xGa_{1-x}As/GaAs$ material used in this work was grown by molecular-beam epitaxy. The substrate is a semi-insulating CZ-grown undoped ⟨100⟩ wafer. The first layer is 12-μm high-quality GaAs buffer layer with 10^{15}-cm^{-3} carrier concentration, the second layer is a 40-Å $Al_xGa_{1-x}As$ ($x = 0.3$) spacer that is followed by a 400-Å Si-doped $Al_xGa_{1-x}As$ ($x = 0.3$) layer with a doping concentration of 2×10^{18} cm^{-3}. This is followed by a 10^{18}-cm^{-3} Si-doped 400-Å GaAs cap layer. In the following experiments, the heating rate was around 0.2 K/s, and they are repeated twice to examine the consistency and reproducibility of the results.

Fig. 6 shows the TAV amplitude as a function of temperature, obtained at dark and under 1.38- and 1.49-eV illumination. Fig. 7 shows the temperature dependencies of the rise times. It can be seen that there is a strong correlation between the amplitude and various time constants associated with the TAV waveform. There are peaks around 100 and 300 K. Under 1.49-eV illumination there are two more peaks: a broad one centered around 170 K and another one around 80 K.

Fig. 6(b) shows a TAV-temperature curve that is obtained under 1.38-eV illumination. Between 150 and 60 K there are three peaks: one at 120 K, another at 100 K, and the third one at 80 K. Fig. 6(b) also shows the effect of SAW power on the TAV-temperature measurement. Large SAW amplitudes yield larger TAV amplitudes making the recording of TAV easier. It also results in a larger overlap between the TAV-T peaks, reducing the resolution of the experiment.

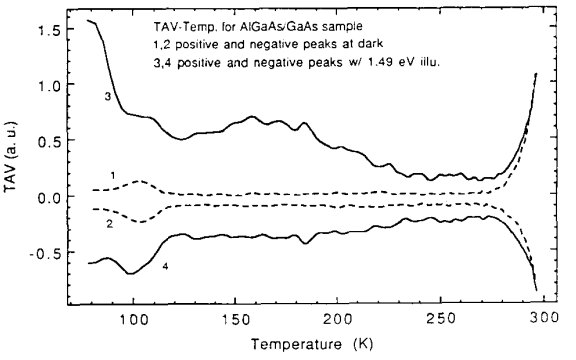

(a)

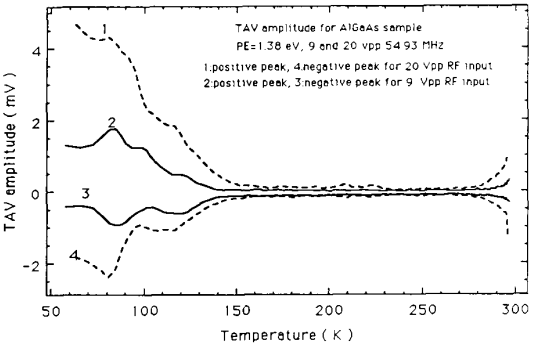

(b)

Fig. 6. TAV versus temperature measurements under different illuminations. (a) At dark and under 1.49-eV illumination. (b) Under 1.38-eV illumination and using different SAW powers.

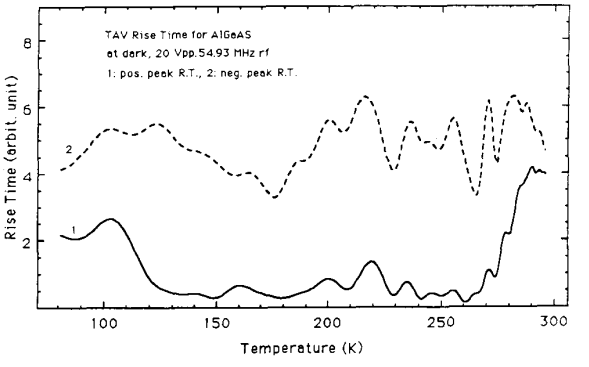

Fig. 7. Transient time constant (τ_1: curve 1 and τ_2: curve 2) versus temperature measurements at dark.

Using (7) and the above experimental values for the temperatures at which TAV maximum occurs, the activation energies shown in Table I are calculated. The majority of the deep levels calculated from TAV peaks are found in bulk CZ-grown GaAs [11], [15]. $Al_xGa_{1-x}As$ layers being only a few hundred Ångstroms, the bulk conductivity is expected to dominate the thermal spectra of TAV.

Fig. 7 shows the variation of the TAV rise times (τ_1 and τ_2, shown in Fig. 4) as a function of temperature at dark. These measurements are also performed under 1.38- and 1.49-eV illumination. The activation energies and trap

TABLE I
ACTIVATION ENERGIES CALCULATED USING (7)

	T_m (K)	E_n (eV)
at dark	100	0.20
	300	0.62
under 1.38 eV ill.	80	0.17
	100	0.20
	120	0.24
	300	0.62
under 1.49 eV ill.	100	0.20
	160	0.33
	300	0.62

TABLE II
ACTIVATION ENERGIES AND APPARENT CROSS SECTIONS CALCULATED FROM FIG. 8

	E_n (eV)	σ_{na} (cm^2)	Point # (figure 8)
at dark	0.15	4×10^{-19}	3
	0.18	3×10^{-18}	2
	0.21	8×10^{-19}	6
	0.27	1×10^{-17}	7
	0.32	5×10^{-16}	4
	0.4	1×10^{-20}	1
	0.41	2×10^{-15}	8
	0.9	7×10^{-6}	5
under 1.49 eV ill.	0.14	4×10^{-19}	
	0.15	4×10^{-19}	
	0.17	8×10^{-19}	
	0.83	2×10^{-19}	
under 1.38 eV ill. SAW =9 V_{pp}	0.12	8×10^{-20}	
	0.25	1×10^{-17}	
	0.37	1×10^{-15}	
	0.37	4×10^{-16}	
	0.6	5×10^{-12}	
under 1.38 eV ill. SAW =20 V_{pp}	0.11	2×10^{-29}	
	0.16	2×10^{-20}	
	0.24	6×10^{-17}	
	0.34	7×10^{-16}	
	0.36	9×10^{-16}	

cross sections, summarized in Table II, are calculated using (8) and (9) and the lifetime data partially shown in Fig. 7. The Arhenius plot constructed using (9) and Fig. 7 is shown in Fig. 8. It is noted that cross sections are assumed to not depend on temperature, and also the γ_n is taken to have the same value in GaAs and $Al_xGa_{1-x}As$.

The 0.413-eV trap with a cross section of 2.43×10^{-15} cm^2 detected at dark also has been reported in vapor phase epitaxy GaAs [15]. The 0.323 eV with a cross section of 5.4×10^{-16} cm^2 is close to the EL7 trap detected in MBE-grown materials [14], [15]. The 0.177-eV trap with a cross

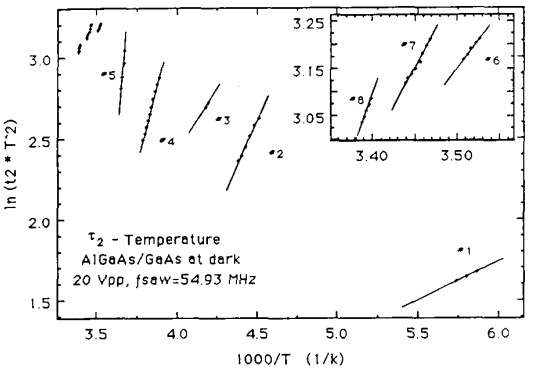

Fig. 8. Arhenius plots constructed using (9) and τ-T experiments. τ_g is the generation lifetime taken to be equal to τ_2 of the TAV waveform shown in Fig. 4 and T is absolute temperature. The trap energies are shown in Table II. (a) At dark. (b) Under 1.49-eV illumination. (c), (d) Under 1.38-eV illumination using different SAW powers.

section of 3.37×10^{-18} cm^2 is close to EL11 except that its apparent cross section detected here is two orders of magnitude smaller than its cross section reported in [15].

The apparent cross sections, in general, are somewhat smaller than the findings of other researchers, except for the 0.876-eV trap detected at dark that has an unreasonably large cross section of 6.6×10^{-6} cm^2. The energy of this level is very close to the energy of the EL2 level in $x = 0.25$ $Al_xGa_{1-x}As$ detected with conventional DLTS [14]. Its cross section, however, is eight orders of magnitude larger than that reported there. This can be attributed to two factors. First, the value of γ_n is different in $Al_xGa_{1-x}As$ than GaAs, and second the electrons released from EL2 in $Al_xGa_{1-x}As$ are spacially separated from these centers and they reside at the interface between the GaAs and $Al_xGa_{1-x}As$. This spacial separation changes the effective mechanism of retrapping from ($Al_xGa_{1-x}As$ conduction-band) to EL2 to (GaAs conduction band) to EL2 reducing the retrapping lifetime. It should also be noticed that the trap energy calculation is less immune to inaccuracies in transient time constant measurements. If the data acquisition system calculates lifetimes with a constant additive error, this error only influences the trap cross section values, not the activation energies.

The trap levels detected under the above bandgap illumination can be related to the ones detected at dark by replacing the Fermi level by quasi-Fermi levels that are determined by the number of photogenerated carriers at any given temperature. The analysis of the trap levels obtained under below bandgap illumination is somewhat more complicated. Using such illumination, electrons from a deep level below the Fermi level can be excited to the conduction band or electrons can be excited from the valence band to the deep levels. These processes change the statistics of occupation of deep levels in a complicated manner. Therefore, the simplifying assumptions that are made in deriving (8) and (9) can no longer be made. In Table II we report the experimental data and the activation energies obtained under various illumination without

analyzing them. A more exact treatment of these results with their analysis will be reported later.

The effect of SAW power can be understood based on the nonlinear nature of the AEI. The larger the SAW power the larger is the accumulation of the semiconductor surface. This results in a slightly larger trap occupancy. In general it is found that, to resolve the trap levels more accurately, that lowest possible SAW power that yields reasonable signal-to-noise ratios should be used. This is shown in Fig. 6(b).

In conclusion, we have applied nondestructive TAV versus temperature measurements to study deep levels in $Al_xGa_{1-x}As/GaAs$ heterostructures. EL2, EL7, and EL11 levels are detected. The activation energies of these levels are in good agreement with values reported in [14] and [15]. Except for the cross section of the EL2 level, which is many orders of magnitude larger than the reported value, the apparent cross sections are in reasonable agreement with the findings of the other researchers.

ACKNOWLEDGMENT

It is a pleasure to thank the Dean's office of Case Western Reserve University for providing an initiation grant to set up the low-temperature system used in this work. All the samples used in the present work were provided by Dr. P. Claspy of CWRU (presently in leave of absence at the NASA Lewis Research Center).

REFERENCES

[1] D. V. Lang, "Deep-level transient spectroscopy: A new method to characterize traps in semiconductors," *J. Appl. Phys.*, vol. 45, no. 7, pp. 3023-3032, 1974.

[2] J. C. Balland, J. P. Zielinger, C. Noguet, and M. Tapiero, "Investigation of deep levels in high-resistivity bulk materials by photo-induced current spectroscopy: I. Review and analysis of some basic problems," *J. Phys. D: Appl. Phys.*, vol. 19, pp. 57-70, 1986.

[3] G. M. Martin, J. Hallais, and G. Poiblaud, "Study of experimental conditions in thermally stimulated current measurements: Application to the characterization of semi insulating chromium-doped gallium arsenide," in *Thermally Stimulated Relaxation in Solids*, P. Braunlinch, Ed. Berlin: Springer Verlag, 1979.

[4] Z. Kachwalla and D. J. Miller, "Transient spectroscopy using the Hall effect," *Appl. Phys. Lett.*, vol. 50, no. 20, p. 1438, 1987.

[5] M. Tabib-Azar, T. Liu, M. N. Abedin, and P. Das, "Characterization of RIE induced radiation damage in silicon using nondestructive transverse acoustoelectric voltage measurements," in *Proc. IEEE Ultrasonics Symp.* (IEEE Pub. 84-CH2112-1), 1984, pp. 926-929.

[6] M. Tabib-Azar, N.-C. Park, and P. Das, "Transient type-inversion of semi-insulating GaAs under illumination at 140 K detected by nondestructive surface acoustic wave technique," *Solid-State Electron.*, vol. 30, no. 7, pp. 705-711, 1987.

[7] M. Tabib-Azar and P. Das, "Nondestructive TAV spectroscopy to detect impurity levels in semiconductor by scanning the energy gap with biasing electric field," *IEEE Ultrasonics Symposium Proc.* (IEEE Pub. 85CH2209-5), 1985, pp. 1016-1921.

[8] M. Tabib-Azar and P. Das, "Acoustoelectric measurements of minority and majority carrier mobilities in semiconductors including $Hg_{1-x}Cd_xTe$," *Appl. Phys. A*, vol. 45, pp. 119-124, 1988.

[9] M. Tabib-Azar, "Characterization of electrical properties of semi-insulating GaAs surface using acousto-electric voltage spectroscopy between 83 K and 300 K with surface wave power as an additional parameter," *Solid-State Electron.*, vol. 31, no. 7, pp. 1197-1204, 1988.

[10] M. Tabib-Azar and P. Das, "Acousto-electric effects in superlattices using separate-medium structure," *Appl. Phys. Lett.*, vol. 50, pp. 436-438, 1987.

[11] M. Tabib-Azar and F. Hajjar, "Deep level transient spectroscopy of Cr-doped GaAs using nondestructive acousto-electric voltage measurement," submitted to *J. Appl. Phys.*

[12] I. J. Fritz, "Transverse acoustoelectric effect in the separate-medium surface-wave configuration," *J. Appl. Phys.*, vol. 52, no. 11, 1981.

[13] A. G. Milnes, *Deep Impurities in Semiconductors.* New York: Wiley, 1973, p. 227.

[14] A. B. Cherifa, R. Azoulay, and G. Guillot, "Properties of the EL2 level in organometallic $Ga_{1-x}Al_xAs$," *Mater. Res. Soc. Symp. Proc.*, vol. 104, pp. 401-404, 1987.

[15] G. M. Martin, A. Mitonneau, and A. Mircea, "Electronic traps in bulk and epitaxial GaAs crystals," *Electron. Lett.*, vol. 13, pp. 191-193, 1977.

*

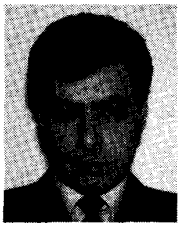

Massood Tabib-Azar (S'83-M'87) was born in Tabriz, Iran, in May 1958. He received the B.S. degree in electrical engineering from Northeastern University in 1980 and the M.S. and Ph.D. degrees in electrical engineering from Rensselaer Polytechnic Institute in 1984 and 1986, respectively. His Master's work was on passivation of GaAs using anodic oxidation, and his Ph.D. work was on characterization of electrical parameters of electronic materials and superlattices using acoustoelectric interaction and other more conventional techniques.

In 1987, he joined Case Western Reserve University as an Assistant Professor. His current research interests include electrical and optical properties of novel materials such as multiple quantum wells and superlattices and modeling of devices fabricated using these materials.

Dr. Tabib-Azar is a member of the APS, the AAPT, and Sigma Xi.

*

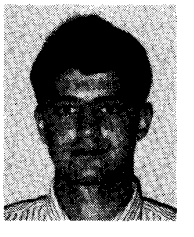

Fares Hajjar was born in Damascus, Syria, in 1965. He received the B.S. and M.S. degrees in electrical engineering in 1987 and 1989, respectively, from Case Western Reserve University, Cleveland, OH.

His current research interests include acoustoelectric interactions in semiconductors, opto-electronics, and noise processes in semiconductor material and devices. He was a guest speaker at the engineer's forum at the Cleveland Engineering Society.

Mr. Hajjar is a member of the National Honor Engineering Society.